

3-(1H-pyrazole-1-yl/1H-1,2,4-triazole-1-yl)-N-propanilide derivatives: Design, Synthesis and Neuroprotectivity Potential Against 6-OHDA Induced Neurotoxicity Model

Ayşe Hande Tarkoğulları Doğan¹, Merve Saylam², Sinem Yılmaz³, Sulunay Parlar¹, Petek Ballar⁴, Vildan Alptuzun¹

¹Department of Pharmaceutical Chemistry, Faculty of Pharmacy, Ege University, Izmir, Turkey

²Department of Pharmaceutical Chemistry, Faculty of Pharmacy, Izmir Katip Celebi University, Izmir, Turkey

³Department of Bioengineering, Faculty of Engineering, University of Alaaddin Keykubat, Antalya, Turkey

⁴Department of Biochemistry, Faculty of Pharmacy, Ege University, Izmir, Turkey

Corresponding Author Information

Ayşe Hande Tarkoğulları Doğan

handeayse@gmail.com

<https://orcid.org/0000-0002-3134-2754>

13.10.2023

17.01.2024

13.02.2024

ABSTRACT

INTRODUCTION: Excessive amounts of neuroapoptosis are the underlying cause of neurodegenerative diseases. Bax is a pro-apoptotic member of the Bcl-2 family that activates caspases which are the members of cysteine protease family that plays significant role in the initiation and execution phases of apoptosis.

In this study, a group of N-propanilide derivatives bearing pyrazole or 1,2,4-triazole ring were designed and synthesized to analyse the neuroprotectivity potential against 6-OHDA and four compounds possessed protectivity at lower doses were subjected to further studies on caspase-3 and Bax pathway.

METHODS: Designed compounds were synthesized by reacting 1H-pyrazole or 1H-1,2,4-triazole with propanilide intermediates in DMF. Neuroprotective activity of the title compounds was analysed against 6-OHDA induced neurotoxicity model. Then, caspase-3 and Bax levels were determined for the selected compounds by Western Blot study.

RESULTS: All twelve 3-(1H-pyrazole-1-yl/1H-1,2,4-triazole-1-yl)-N-propanilide derivatives possessed neuroprotectivity against 6-OHDA induced neurotoxicity model. Compounds 7, 10, 11, and 12 were found to be more active at lower doses also, therefore, they were subjected to further studies and the results revealed that their protecting activity arise from the decreasing the levels of Bax, one of the pro-apoptotic proteins, and c expression levels and caspase-3 proteins.

DISCUSSION AND CONCLUSION: All designed and synthesized derivatives possessed neuroprotectivity against 6-OHDA induced neurotoxicity in SH-SY5Y cell line and compounds 7, 10, 11, and 12 revealed that their neuroprotectivity is originated from the decreasing the bax expression levels and caspase-3 activation.

Keywords: neuroprotectivity, caspase-3, Bax protein, 1, 2, 4-triazole, 1H-pyrazole

INTRODUCTION

Physiologically, cell proliferation and cell death should be in multicellular organisms ¹. Apoptosis is a programmed cell death process that is characterized by biochemical and morphological changes in cells leading eventually to cell death ². Central to the execution of apoptosis is a group of proteolytic enzymes known as caspases which are cysteine proteases. Recently, there are 14 members of the caspase family and 11 of them are found in humans ^{3,4}. Caspases operate the apoptosis process both directly and indirectly ⁴. Especially, caspase-3 stands as one of the principal effectors in the initiation and execution phases of apoptosis. Once caspase-3 is activated in the cell, it cleaves a wide range of substrates, leading to biochemical and morphological changes associated with apoptosis ⁵.

Bcl-2 (proteins of the B-cell lymphoma-2) and the mitochondrial pathway are critical intermediates in this pathway, one of the four major pathways that lead to caspase activation ⁵. When cells get apoptotic signals; Bax which is a pro-apoptotic protein and belongs to the Bcl-2 family, undergoes a multistep process to trigger the activation of caspases to execute the apoptotic program leading to cell death ^{2,4,5}.

Neuronal cells have different cycle than the other cells as they live longer to maintain their routine pathways ⁶. Sometimes, redundant amounts and rate of neuronal apoptosis (neuroapoptosis) take place and trigger such neurodegenerative diseases as Parkinson's disease (PD), Alzheimer's disease (AD), multiple sclerosis (MS), and amyotrophic lateral sclerosis (ALS) ^{3,7}.

Based on these findings, it is suggested that triggering apoptosis with the increase of caspase-3 and Bax plays a significant role in the pathogenesis of neurological disorders. Therefore, inhibition of 6-OHDA-induced neurodegeneration and inhibition of the activated caspases may be counted as an important target on the treatment of neurodegenerative diseases.

We have reported cholinesterase activity of a group of N-propanilide derivatives bearing pyrazole or 1,2,4-triazole ring and investigated the neuroprotectivity potential of the most active derivatives in our previous studies ⁸. Based on the promising results

on neuroprotectivity and cholinesterase inhibition, we designed *N*-propananilide derivatives bearing pyrazole or 1,2,4-triazole ring and their cholinesterase activity was tested, but the results were negligible, therefore, we have decided to focus on their neuroprotective activities. We have tested the neuroprotective potential of the synthesized compounds in SH-SY5Y neurotoxicity model induced by 6-OHDA (6-hydroxydopamine) which is a neurotoxic agent, which is used for neurotoxicity assays based on its ability to be autoxidized to yield potentially toxic products and reactive oxygen species (ROS) ⁹. Then, we have further analysed the underlying mechanism by immunoblotting studies for caspase-3 and Bax proteins for the most active ones.

MATERIALS AND METHODS

Thin-layer chromatography (TLC) was processed on silica gel plates (Merck, Kieselgel 60F254) and detected by 254 nm UV light. The structures of the compounds were verified by using IR spectra (Perkin Elmer FT-IR Spectrometer 100 with ATR attachment, Perkin Elmer Inc., Massachusetts, USA), Mass spectra (APCI-ESI), (Thermo MSQ Plus LC/MS, Thermoscientific Inc., San Jose, CA, USA) and NMR spectra (Varian As 400 Mercury Plus NMR, Varian Inc., Palo Alto, CA, USA). Melting points were determined by using melting point apparatus on Stuart SMP30 and are uncorrected. Elemental analysis was verified on TruSpec Micro Instrument LECO CHNS 932. All the used starting materials and reagents for synthesis were commercial products with high-grade properties.

General procedure for the synthesis of the compounds **1a-6a**

Substituted aniline (1 eq.) and K₂CO₃ (1 eq.) were dissolved in the mixture of acetone:water (1:2). 3-chloropropionyl chloride (1 eq.) was added in ice bath drop by drop and the mixture was stirred at room temperature for 2 hours. Then, the reaction mixture was poured into cold water, the precipitate was filtered and washed with water ¹⁰.

General procedure for the synthesis of the compounds **1-12**

ω -Chloro-*N*-propananilides (1 eq.), pyrazole or triazole (1 eq.) and K₂CO₃ (1 eq.) were dissolved in DMF and allowed to react under reflux. After monitoring the end of the reaction, DMF was evaporated under reduced pressure and the residue was extracted with chloroform and water. Organic phases were evaporated after drying over anhydrous Na₂SO₄ ¹¹. Crude products were purified on column chromatography with various mobile phases.

N-(2-chlorophenyl)-3-(1*H*-pyrazol-1-yl)propanamide (1)

Yield, 30 %; m.p., 102 °C; IR (ATR) ν_{max} (cm⁻¹): 3279 (NH), 1650 (amide I), 1533 (amide II); ¹H NMR (CDCl₃, 400 MHz) δ 3.04 (t, 2H, *J*=6.3 Hz, CH₂), 4.53 (t, 2H, *J*=6.3 Hz, CH₂), 6.21 (t, 1H, *J*=2.1 Hz, Py-H), 7.03 (td, 1H, *J*=7.8; 1.6 Hz, Ph-H), 7.22-7.26 (m, 1H, Ph-H), 7.33 (dd, 1H, *J*=8.1; 1.5 Hz, Ph-H), 7.45 (d, 1H, *J*=2.3 Hz, Py-H), 7.54 (d, 1H, *J*=1.5 Hz, Py-H), 7.91 (brs, 1H, NH), 8.27 (d, 1H, *J*=8.3 Hz, Ph-H) ppm; MS (ESI) *m/z* (% intensity): 123 (100), 250 (73) [M+H]⁺, 252 (23) [M+2+H]⁺; Anal. Calcd for C₁₂H₁₂ClN₃O (249): C: 57.72; H: 4.84; N: 16.83. Found C: 57.60; H: 4.99; N: 16.42.

N-(3-chlorophenyl)-3-(1*H*-pyrazol-1-yl)propanamide (2)

Yield, 72 %; m.p., 76 °C; IR (ATR) ν_{max} (cm⁻¹): 3236 (NH), 1685 (amide I), 1590 (amide II); ¹H NMR (CDCl₃, 400 MHz) δ 2.95 (t, 2H, *J*=6.1 Hz, CH₂), 4.51 (t, 2H, *J*=6.1 Hz, CH₂), 6.25 (t, 1H, *J*=2.1 Hz, Py-H), 7.04-7.07 (m, 1H, Ph-H), 7.19 (t, 1H, *J*=8.0 Hz, Ph-H), 7.26-7.29 (m, 1H, Ph-H), 7.46 (d, 1H, *J*=2.3 Hz, Py-H), 7.57-7.64 (m, 2H, Ph-H and Py-H), 8.53 (brs, 1H, NH) ppm; MS (APCI) *m/z* (% intensity): 250 (100) [M+H]⁺, 252 (23) [M+2+H]⁺; Anal. Calcd for C₁₂H₁₂ClN₃O (249): C: 57.72; H: 4.84; N: 16.83. Found C: 57.38; H: 5.07; N: 16.46.

N-(4-chlorophenyl)-3-(1*H*-pyrazol-1-yl)propanamide (3)

Yield, 59 %; m.p., 151 °C; IR (ATR) ν_{max} (cm⁻¹): 3246 (NH), 1677 (amide I), 1538 (amide II); ¹H NMR (CDCl₃, 400 MHz) δ 2.83 (t, 2H, *J*=6.4 Hz, CH₂), 4.40 (t, 2H, *J*=6.4 Hz, CH₂), 6.09-6.10 (m, 1H, Py-H), 7.09-7.13 (m, 2H, Ph-2H), 7.36-7.42 (m, 4H, Ph-2H and Py-2H), 9.25 (brs, 1H, NH) ppm; MS (APCI) *m/z* (% intensity): 123 (97), 250 (100) [M+H]⁺, 252 (32) [M+2+H]⁺; Anal. Calcd for C₁₂H₁₂ClN₃O (249): C: 57.72; H: 4.84; N: 16.83. Found C: 57.52; H: 4.88; N: 16.50.

N-(2-methoxyphenyl)-3-(1*H*-pyrazol-1-yl)propanamide (4)

Yield, 62 %; m.p., 88 °C; IR (ATR) ν_{max} (cm⁻¹): 3374 (NH), 1681 (amide I), 1534 (amide II); ¹H NMR (CDCl₃, 400 MHz) δ 2.98 (t, 2H, *J*=6.5 Hz, CH₂), 3.83 (s, 3H, OCH₃), 4.53 (t, 2H, *J*=6.5 Hz, CH₂), 6.19 (t, 1H, *J*=2.1 Hz, Py-H), 6.84 (dd, 1H, *J*=8.1; 1.4 Hz, Ph-H), 6.91-6.95 (m, 1H, Ph-H), 7.03 (td, 1H, *J*=7.8; 1.7 Hz, Ph-H), 7.45-7.46 (m, 1H, Py-H), 7.51-7.52 (m, 1H, Py-H), 7.84 (brs, 1H, NH), 8.29-8.31 (m, 1H, Ph-H) ppm; MS (APCI) *m/z* (% intensity): 123 (100), 246 (86) [M+H]⁺; Anal. Calcd for C₁₃H₁₅N₃O₂ (245): C: 63.66; H: 6.16; N: 17.13. Found C: 63.30; H: 6.48; N: 16.84.

N-(3-methoxyphenyl)-3-(1*H*-pyrazol-1-yl)propanamide (5)

Yield, 66 %; m.p., 96 °C; IR (ATR) ν_{max} (cm⁻¹): 3262 (NH), 1692 (amide I), 1491 (amide II); ¹H NMR (CDCl₃, 400 MHz) δ 2.94 (t, 2H, *J*=6.1 Hz, CH₂), 3.78 (s, 3H, OCH₃), 4.51 (t, 2H, *J*=6.2 Hz, CH₂), 6.23 (t, 1H, *J*=2.1 Hz, Py-H), 6.62-6.65 (m, 1H, Ph-H), 6.91 (d, 1H, *J*=7.8 Hz, Ph-H), 7.15-7.19 (m, 2H, Ph-2H), 7.45 (dd, 1H, *J*=2.3; 0.7 Hz, Py-H), 7.55-7.56 (m, 1H, Py-H), 8.14 (brs, 1H, NH) ppm; MS (APCI) *m/z* (% intensity): 246 (100) [M+H]⁺; Anal. Calcd for C₁₃H₁₅N₃O₂ (245): C: 63.66; H: 6.16; N: 17.13. Found C: 63.70; H: 6.24; N: 16.70.

N-(4-methoxyphenyl)-3-(1*H*-pyrazol-1-yl)propanamide (6)

Yield, 14 %; m.p., 127 °C; IR (ATR) ν_{max} (cm⁻¹): 3297 (NH), 1654 (amide I), 1529 (amide II); ¹H NMR (CDCl₃, 400 MHz) δ 2.91 (t, 2H, *J*=6.2 Hz, CH₂), 3.77 (s, 3H, OCH₃), 4.51 (t, 2H, *J*=6.2 Hz, CH₂), 6.23 (t, 1H, *J*=2.1 Hz, Py-H), 6.82 (d, 2H, *J*=9.0 Hz, Ph-2H), 7.31 (d, 2H, *J*=9.0 Hz, Ph-2H), 7.45 (d, 1H, *J*=2.3 Hz, Py-H), 7.55 (d, 1H, *J*=1.9 Hz, Py-H), 7.93 (brs, 1H, NH) ppm; MS (APCI) *m/z* (% intensity): 178 (100), 246 (91) [M+H]⁺; Anal. Calcd for C₁₃H₁₅N₃O₂ (245): C: 63.66; H: 6.16; N: 17.13. Found C: 63.25; H: 5.98; N: 16.83.

N-(2-chlorophenyl)-3-(1*H*-1,2,4-triazol-1-yl)propanamide (7)

Yield, 7 %; m.p., 98 °C; IR (ATR) ν_{max} (cm⁻¹): 3129 (NH), 1691 (amide I), 1507 (amide II); ¹H NMR (CDCl₃, 400 MHz) δ 3.04 (t, 2H, *J*=6.2 Hz, CH₂), 4.59 (t, 2H, *J*=6.2 Hz, CH₂), 7.03-7.07 (m, 1H, Ph-H), 7.23-7.27 (m, 1H, Ph-H), 7.34 (dd, 1H, *J*=8.1; 1.5 Hz, Ph-H), 7.67 (brs, 1H, NH), 7.95 (s, 1H, Tr-H), 8.17 (s, 1H, Tr-H), 8.24 (d, 1H, *J*=8.4 Hz, Ph-H) ppm; MS (ESI) *m/z* (% intensity):

251 (100) [M+H]⁺, 253 (30) [M+2+H]⁺; Anal. Calcd for C₁₁H₁₁ClN₄O (250): C: 52.70; H: 4.42; N: 22.35. Found C: 52.79; H: 4.79; N: 22.18.

N-(3-chlorophenyl)-3-(1*H*-1,2,4-triazol-1-yl)propanamide (8)

Yield, 38 %; m.p., 167 °C; IR (ATR) ν_{max} . (cm⁻¹): 3122 (NH), 1690 (amide I), 1540 (amide II); ¹H NMR (CDCl₃, 400 MHz) δ 2.82 (t, 2H, *J*=6.3 Hz, CH₂), 4.42 (t, 2H, *J*=6.3 Hz, CH₂), 6.86-6.89 (m, 1H, Ph-H), 7.05 (t, 1H, *J*=8.1 Hz, Ph-H), 7.24-7.27 (m, 1H, Ph-H), 7.53 (t, 1H, *J*=2.0 Hz, Ph-H) 7.76 (s, 1H, Tr-H), 8.06 (s, 1H, Tr-H), 9.47 (brs, 1H, NH) ppm; MS (APCI) *m/z* (% intensity): 251 (100) [M+H]⁺, 253 (29) [M+2+H]⁺; Anal. Calcd for C₁₁H₁₁ClN₄O (250): C: 52.70; H: 4.42; N: 22.35. Found C: 52.77; H: 4.49; N: 21.98.

N-(4-chlorophenyl)-3-(1*H*-1,2,4-triazol-1-yl)propanamide (9)

Yield, 59 %; m.p., 136 °C; IR (ATR) ν_{max} . (cm⁻¹): 3124 (NH), 1697 (amide I), 1547 (amide II); ¹H NMR (CDCl₃, 400 MHz) δ 2.95 (t, 2H, *J*=6.1 Hz, CH₂), 4.57 (t, 2H, *J*=6.1 Hz, CH₂), 7.26 (d, 2H, *J*=8.8 Hz, Ph-2H), 7.38 (d, 2H, *J*=8.8 Hz, Ph-2H), 7.62 (brs, 1H, NH), 7.95 (s, 1H, Tr-H), 8.16 (s, 1H, Tr-H) ppm; MS (ESI) *m/z* (% intensity): 249 (100) [M-H]⁻, 253 (28) [M+2-H]⁻; Anal. Calcd for C₁₁H₁₁ClN₄O (250): C: 52.70; H: 4.42; N: 22.35. Found C: 52.79; H: 4.37; N: 22.05.

N-(2-methoxyphenyl)-3-(1*H*-1,2,4-triazol-1-yl)propanamide (10)

Yield, 84 %; m.p., 81 °C; IR (ATR) ν_{max} . (cm⁻¹): 3112 (NH), 1688 (amide I), 1537 (amide II); ¹H NMR (CDCl₃, 400 MHz) δ 2.99 (t, 2H, *J*=6.2 Hz, CH₂), 3.84 (s, 3H, OCH₃), 4.58 (t, 2H, *J*=6.3 Hz, CH₂), 6.84 (dd, 1H, *J*=8.1; 1.4 Hz, Ph-H), 6.93 (td, 1H, *J*=7.8; 1.4 Hz, Ph-H), 7.04 (td, 1H, *J*=7.8; 1.7 Hz, Ph-H), 7.75 (brs, 1H, NH), 7.93 (s, 1H, Tr-H), 8.16 (s, 1H, Tr-H), 8.25 (dd, 1H, *J*=8.1; 1.6 Hz, Ph-H) ppm; MS (ESI) *m/z* (% intensity): 247 (100) [M+H]⁺; Anal. Calcd for C₁₂H₁₄N₄O₂ (246): C: 58.53; H: 5.73; N: 22.75. Found C: 58.11; H: 5.88; N: 22.51.

N-(3-methoxyphenyl)-3-(1*H*-1,2,4-triazol-1-yl)propanamide (11)

Yield, 33 %; m.p., 152 °C; IR (ATR) ν_{max} . (cm⁻¹): 3114 (NH), 1675 (amide I), 1555 (amide II); ¹H NMR (CDCl₃, 400 MHz) δ 2.79 (t, 2H, *J*=6.4 Hz, CH₂), 3.62 (s, 3H, OCH₃), 4.40 (t, 2H, *J*=6.4 Hz, CH₂), 6.44-6.46 (m, 1H, Ph-H), 6.86-6.89 (m, 1H, Ph-H), 7.00 (t, 1H, *J*=8.1 Hz, Ph-H), 7.12 (t, 1H, *J*=2.2 Hz, Ph-H), 7.74 (s, 1H, Tr-H), 8.05 (s, 1H, Tr-H), 9.23 (brs, 1H, NH), ppm; MS (ESI) *m/z* (% intensity): 247 (100) [M+H]⁺; Anal. Calcd for C₁₂H₁₄N₄O₂ (246): C: 58.53; H: 5.73; N: 22.75. Found C: 58.35; H: 5.71; N: 22.41.

N-(4-methoxyphenyl)-3-(1*H*-1,2,4-triazol-1-yl)propanamide (12)

Yield, 49 %; m.p. 129 °C; IR (ATR) ν_{max} . (cm⁻¹): 3113 (NH), 1682 (amide I), 1557 (amide II); ¹H NMR (CDCl₃, 400 MHz) δ 2.90 (t, 2H, *J*=6.2 Hz, CH₂), 3.76 (s, 3H, OCH₃), 4.55 (t, 2H, *J*=6.2 Hz, CH₂), 6.81 (d, 2H, *J*=9.0 Hz, Ph-2H), 7.29 (d, 2H, *J*=9.0 Hz, Ph-2H), 7.67 (brs, 1H, NH), 7.93 (s, 1H, Tr-H), 8.15 (s, 1H, Tr-H), 8.25 (dd, 1H, *J*=8.1; 1.6 Hz, Ph-H) ppm; MS (ESI) *m/z* (% intensity): 178 (29), 247 (100) [M+H]⁺; Anal. Calcd for C₁₂H₁₄N₄O₂ (246): C: 58.53; H: 5.73; N: 22.75. Found C: 58.40; H: 5.72; N: 22.34.

Cell lines and treatments

SH-SY5Y cell line (human dopaminergic neurons), obtained from ATCC, was maintained in DMEM (Dulbecco's modified Eagle's medium; Biological Ind., Israel) involving %10 FBS (fetal bovine serum, Panbiotech, Germany) and 2 mM L-glutamine (Biological Ind., Israel) according to the instruction guideline. While cells were seeded at a density of 2x10⁴ cells per well for cell viability assay; for Western blot study cell were seeded at 5x10⁵ per well. The day after, cells were pre-treated with desired concentrations of synthesized compounds for 12 h then treated with 50 μ m 6-OHDA (Sigma Aldrich, UK) for 12 h. DMSO-treated cells were used as a negative experimental control.

While 6-OHDA was prepared in sterile water as 1000X stock solution, the synthesized compounds were prepared in DMSO. The DMSO final concentration was below % 0.1.

Cell viability assay

The potential neuroprotection properties of synthesised compounds against 6-OHDA induced neurotoxicity were assessed via WST reagent (Roche, Switzerland) according to the manufacturer's instructions. Cell viability assay was performed via replacing the old media with WST/medium mixture (1:9). The measurement of absorbance was done with a microplate reader at 440 nm and 690 nm (Varioscan, Thermo Fisher Scientific, US). The viability of cells was presented as percentage of cell viability compared to DMSO-treated cells. This experiment was conducted by triplicate.

Western Blot (WB) study

Cells were harvested with RIPA buffer involving protease inhibitors cocktails (Roche, Switzerland). The bicinchoninic acid (BCA, Thermo Fisher Scientific, US) protein assay was used to determine total protein levels according to the manufacturer's instructions. Equal amount of protein was used for WB studies. After denaturation of protein samples in 4X Laemmli buffer (Bio-Rad, US) at 95 °C for 5 min, the samples were first separated via SDS-PAGE electrophoresis then transferred to PDVF membranes EMD Millipore, Thermo Fisher Scientific, US). Next, the membranes were blocked with blocking buffer (PBS-0.1% Tween-20 with 5% non-fat dry milk). In this study, while anti-actin (1:10000, Sigma-Aldrich-A5316, UK) was used as mouse monoclonal antibody, antibodies anti-caspase-3 (1:3000, CST-9665, US) and anti-bax (1:3000, CST-2774, US) were used as rabbit monoclonal antibodies. Besides,

Goat anti-rabbit (1:5000, Thermo Fisher Scientific-31460, US) and Goat anti-mouse (1:5000, Thermo Fisher Scientific-31430, US) antibodies were used as secondary antibodies. Fusion-FX7 (Vilber Lourmat, Thermo Fisher Scientific, USA) and Clarity ECL substrate solution (Bio-Rad, USA) were used to determine the chemiluminescence signal.

Statistical analysis

Data were shown as means \pm standard deviation (SD). The experiment was conducted with three independent biological replicates with two technical replicates. Student t-test was used to determine the significance of differences between groups (** $p \leq 0.001$, *** $p \leq 0.005$).

AChE activity

AChE enzyme activity was investigated with slight modifications of Ellman et al.^{12,13}. Thiocoline, the product of the enzymatic hydrolysis, does not have a distinct chromophore for UV detection, therefore 5,5'-Dithiobis(2-nitrobenzoic acid) [Ellman's reagent, DTNB, Sigma-Aldrich, (St. Louis, MO, USA)] was used for the evaluation of enzyme activity. All compounds were tested at 30 μM and 300 μM concentrations. Galantamine was used as a positive control. Each concentration was studied three times. All solutions were adjusted to 20°C before use. First, 3.0 ml of phosphate buffer (0.1 M; pH 8.0), then 100 μl of substrate solution (dissolved in 2% DMSO and then diluted to lower than 0.2% DMSO in the aqueous assay medium), 100 μl of enzyme solution [2.5 units/ μl] (from electric eel, E.C.3.1.1.7., Type VI-S, Sigma-Aldrich) was added into the cuvette and incubated for 5 min. After required fractional amounts of the DTNB solution (0.01 M, 100 ml) and 20 μl of the ATC (0.075 M) were also added, the cuvette was mixed immediately and rapidly. Enzymatic hydrolysis of ATC was detected at 412 nm by UV-visible absorption (Shimadzu UV/160-A spectrophotometer). The *in vitro* results for AChE are given in Table 1.

RESULTS AND DISCUSSION

Chemistry

In this study, twelve substituted *N*-propanilide derivatives bearing pyrazole or 1,2,4-triazole were synthesized^{10,11}. After the acylation of substituted anilines with 3-chloropropionyl chloride (compounds **1a-6a**), they were reacted with pyrazole or 1,2,4-triazole in DMF to form **1-6** and **7-12**, respectively (Scheme 1). While the structures of final compounds were verified by spectral methods, purity percentages were determined by elemental analysis. Strong stretching bands were noticed regarding the carbonyl group at 1697-1650 cm^{-1} and 1590-1491 cm^{-1} as amide I band and amide II band, respectively (Supplementary material). Also stretching signals in the H bond region (3374-3112 cm^{-1}) verifying the existence of amide functional group were observed^{14,15}.

The chemical shifts and coupling constants of ¹H NMR spectra were in total agreement with molecular structures. While the signals of methylene protons neighbouring carbonyl group were observed at δ 2.79 - δ 3.04, signals of methylene protons neighbouring heterocyclic ring systems were observed at δ 4.40 - δ 4.59 region because the deshielding effect of pyrazole/1,2,4-triazole rings are more than the deshielding effect of the carbonyl functional group¹⁶. NH proton of the amide function was noticed as broad singlet from δ 7.50 to 9.50 depending on the position and types of substituents (Supplementary material).

The mass spectra of the title compounds were recorded by using ESI or APCI techniques. $[M+1]^+$ and $[M-1]^-$ signals were determined regarding the molecular weights. Additionally, the expected molecular formulas and purity of the compounds were supported within $\pm 0.4\%$ range by the elemental analysis results (Supplementary material).

All the molecules except **10** have registry numbers but no corresponding scientific data is available.

Neuroprotective effects of the final compounds against neurotoxicity

Potential neuroprotective activity of the title compounds was analysed against 6-OHDA induced neurotoxicity model. First, cells were pre-treated with desired concentrations of compounds (1, 5, 10, 25 and 50 μM) for 12 h; then they were subjected to 6-OHDA treatment for another 12 h. The cell viability assays, performed by WST-1 reagent, showed that all final compounds possessed remarkable neuroprotective effect against 6-OHDA induced cells and compounds **1**, **5**, **7**, **10**, and **12** reduced the toxic effect of 6-OHDA more effectively at lower doses. 6-OHDA treatment decreased the cell viability by $46.30 \pm 0.66\%$ (Figure 1). The viabilities were revitalized to the extent of 74.40 ± 0.76 , and $70.09 \pm 1.44\%$ at 1 and 5 concentrations of compound **1**, respectively. The highest dose of compound **1** did not reverse the cell viability as much as its lower concentrations. Compound **5** treatment increased the cell viability to 98.78 ± 2.23 and $99.68 \pm 4.04\%$ at the 5 and 10 μM concentrations, respectively. While compound **7** treatment ameliorated the cell viability to 104.33 ± 3.77 and $111.12 \pm 3.02\%$ at the 1 and 5 μM concentrations, respectively; compound **10** increased the cell viability to 101.97 ± 3.11 and $107.54 \pm 2.25\%$ at the 1 and 5 μM concentrations, respectively. Compound **12**, another synthesized molecule that increased cell viability at lower doses, enhanced the viability up to the concentration of 10 μM (103.07 ± 2.24 , 106.49 ± 2.59 , $113.69 \pm 2.14\%$ at the 1, 5, and 10 μM concentration, respectively). The treatments of compounds **2**, **6**, and **11** performed the cell viability in a dose-dependent manner which means that the highest doses (50 μM) did not show any cytotoxic effect on SH-SY5Y cells ($101.98 \pm 1.97\%$ for 50 μM concentration of compound **2**, $102.21 \pm 2.26\%$ for 50 μM concentration of compound **6**, $104.35 \pm 2.26\%$ for 50 μM concentration of compound **11**). Compound **3** increased the cell viability up to a concentration of 25 μM in a dose-dependent manner. The viability was decreased dramatically to $69.09 \pm 0.98\%$ at the highest concentration, which may be due to the cytotoxic effect of the highest dose of this compound. While compound **4** increased the cell viability up to a concentration of 25 μM ($98.60 \pm 3.51\%$), it was shown a minor decreased at 50 μM concentration ($93.36 \pm 3.38\%$). Also, the treatment of compound **9** triggered cell viability in a dose dependent manner up to a concentration of 10 μM , then it was shown that a minor and moderate decrease at higher concentration ($92.95 \pm 0.90\%$ at 25 μM and $79.20 \pm 1.95\%$ at 50 μM). Finally, compound **8** did not increase the cell viability at lower dose whereas the treatments of higher doses attenuated 6-OHDA toxicity at higher doses ($113.02 \pm 4.73\%$, $111.03 \pm 1.48\%$ and $111.20 \pm 5.20\%$ at 10-, 25 and 50 μM , respectively) (Figure 1) (Supplementary Material).

Protective effects of the final compounds against cell death

6-OHDA is used in neurotoxicity model for Parkinson both *in vitro* and *in vivo*¹⁷ based on its trigger effect to activate caspase-3 and increase the level of Bax protein in several studies¹⁸⁻²⁰.

Based on the significant neuroprotective activity of the final compounds, we have selected compounds **7**, **10**, **11**, and **12** for further studies as they also displayed impressive neuroprotectivity at lower doses. For this purpose, we used the same experimental condition as in the cell viability assays. Consistent with the literature, alone treatment of 6-OHDA increased the level of Bax and

cleavage caspase-3 proteins levels. This increase in Bax and cleave caspase-3 was significantly attenuated in cells pre-treated with compounds **7**, **10**, **11**, and **12** (Figure 2). 6-OHDA, 6-hydroxylated analogue of dopamine, causes degeneration of dopaminergic neurons. Treatment of 6-OHDA induces cellular damage through a reaction with nucleophiles such as protein and DNA and lead to apoptotic cell death²¹. Our results revealed that compounds **7**, **10**, **11**, and **12** protect SH-SY5Y cells from 6-OHDA toxicity by decreasing pro-apoptotic Bax expression levels and caspase-3 activation.

AChE activity

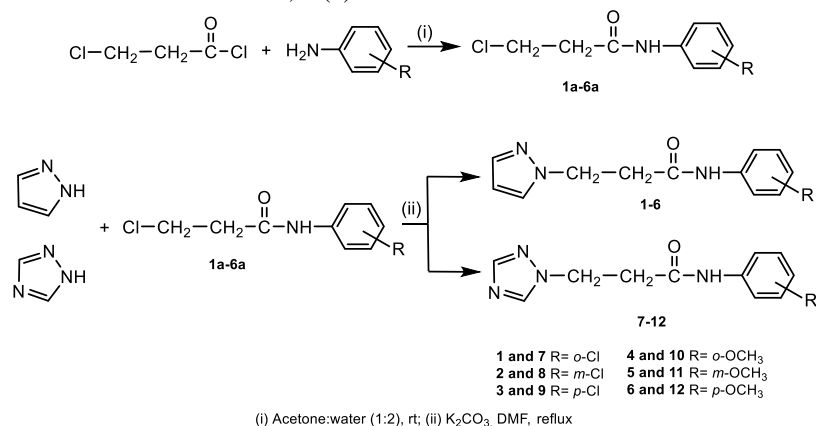
All compounds were screened for AChE inhibitory potential by using Ellman's slightly modified colorimetric method and Galantamine was the standard drug^{12,22}. The results showed that all the synthesized compounds possessed weak AChE inhibitory activity (Table 1). As shown in table 1, the title compounds exhibited 64.4-86.2% inhibition at 300 μ M and 13.62-30.22% inhibition at 30 μ M on AChE. Among the series, compounds **7**, **10** and **12** have better activity than the other tested compounds at both concentrations. Especially, compound **12** named *N*-(4-methoxyphenyl)-2-(1*H*-1,2,4-triazol-1-yl)propanamide, was found to be the most potent derivative of all the synthesized derivatives, with an 86.2% inhibition at 300 μ M and an 30.2% inhibition at 30 μ M on AChE (Table 1).

CONCLUSION

In this study, we have designed and synthesized twelve substituted *N*-propananilide derivatives bearing pyrazole or 1,2,4-triazole ring based on the neuroprotectivity results of the compounds of our previous study⁸. In terms of the neuroprotective potential, generally triazole derivatives possess better activity than the pyrazole derivatives. Furthermore, compounds, which have potential against AChE, have neuroprotective effects. Additionally, compounds **7**, **10**, **11**, and **12** present neuroprotection against 6-OHDA-induced neurotoxicity via decreasing pro-apoptotic protein Bax and cleaved caspase-3 which has a central role in cellular apoptosis. In conclusion, we can state that adding one methylene group to the linker increases the neuroprotective effect of the designed compounds but decreases the AChE inhibitory activity, therefore, adding one more methylene group to the intermediate chain to test the neuroprotective activity of the pyrazole/1,2,4-triazole butyramide derivatives will be our future scope.

1. Vitale I, Pietrocola F, Guilbaud E, et al. Apoptotic cell death in disease—Current understanding of the NCCD 2023. *Cell Death Differ.* 2023;30(5):1097-1154. doi:10.1038/s41418-023-01153-w
2. Mattson MP. Apoptosis in neurodegenerative disorders. *Nat Rev Mol Cell Biol.* 2000;1(2):120-130. doi:10.1038/35040009
3. Radi E, Formichi P, Battisti C, Federico A. Apoptosis and oxidative stress in neurodegenerative diseases. Korczyn AD, ed. *J Alzheimer's Dis.* 2014;42(s3):S125-S152. doi:10.3233/JAD-132738
4. Friedlander RM. Apoptosis and Caspases in neurodegenerative diseases. *N Engl J Med.* 2003;348(14):1365-1375. doi:10.1056/nejmra022366
5. McDonald ES, Windebank AJ. Mechanisms of neurotoxic injury and cell death. *Neurol Clin.* 2000;18(3):525-540. doi:10.1016/S0733-8619(05)70209-7
6. Fricker M, Tolkovsky AM, Borutaite V, Coleman M, Brown GC. Neuronal cell death. *Physiol Rev.* 2018;98(2):813-880. doi:10.1152/physrev.00011.2017
7. Cacciatore I, Fornasari E, Baldassarre L, et al. A potent (R)-alpha-bis-lipoyl derivative containing 8-hydroxyquinoline scaffold: Synthesis and biological evaluation of its neuroprotective capabilities in SH-SY5Y Human Neuroblastoma Cells. *Pharmaceuticals.* 2013;6(1):54-69. doi:10.3390/ph6010054
8. Saylam M, Tarikogullari AH, Yilmaz S, Ballar Kırmızıbayrak P. Neuroprotective activity studies of some phenylacetamide derivatives bearing 1*H*-pyrazole or 1*H*-1,2,4-triazole. *Bioorganic Med Chem Reports.* 2022;2(2):1-5. doi:10.25135/acg.bmc.26.2111.2255
9. Varešlija D, Tipton KF, Davey GP, McDonald AG. 6-Hydroxydopamine: a far from simple neurotoxin. *J Neural Transm.* 2020;127(2):213-230. doi:10.1007/s00702-019-02133-6
10. Ren JL, Zhang XY, Yu B, et al. Discovery of novel AHLs as potent antiproliferative agents. *Eur J Med Chem.* 2015;93:321-329. doi:10.1016/j.ejmech.2015.02.026
11. Bonfanti JF, Doublet F, Fortin J, et al. Selection of a respiratory syncytial virus fusion inhibitor clinical candidate, Part 1: Improving the pharmacokinetic profile using the structure–property relationship. *J Med Chem.* 2007;50(19):4572-4584. doi:10.1021/jm070143x
12. Ellman GL, Courtney KD, Andres V, Featherstone RM. A new and rapid colorimetric determination of acetylcholinesterase activity. *Biochem Pharmacol.* 1961;7(2):88-95. doi:10.1016/0006-2952(61)90145-9
13. Kapková P, Stiefl N, Sürig U, Engels B, Baumann K, Holzgrabe U. Synthesis, biological activity, and docking studies of new Acetylcholinesterase inhibitors of the Bispyridinium type. *Arch Pharm (Weinheim).* 2003;336(11):523-540. doi:10.1002/ardp.200300795
14. Robert M. Silverstein, Webster FX, Kiemle DJ, Bryce DL. Spectrometric Identification of Organic Compounds, 8th Edition. Published online 2014:2014.
15. Nakanishi K, Solomon PA. Infrared Absorption Spectroscopy. 2nd Edition. Published online 1977:287.
16. Hesse M, Meier H, Zeeh B. Spectroscopic Methods in Organic Chemistry, 2nd Edition 2007. Published online 2007:450.
17. Lou H, Jing X, Wei X, Shi H, Ren D, Zhang X. Naringenin protects against 6-OHDA-induced neurotoxicity via activation of the Nrf2/ARE signaling pathway. *Neuropharmacology.* 2014;79:380-388. doi:10.1016/j.neuropharm.2013.11.026
18. Gomez-Lazaro M, Galindo MF, Concannon CG, et al. 6-Hydroxydopamine activates the mitochondrial apoptosis pathway through p38 MAPK-mediated, p53-independent activation of Bax and PUMA. *J Neurochem.* 2008;104(6):1599-1612. doi:10.1111/j.1471-4159.2007.05115.x

19. Jordán J, Galindo MF, Tornero D, González-García C, Ceña V. Bcl-xL blocks mitochondrial multiple conductance channel activation and inhibits 6-OHDA-induced death in SH-SY5Y cells. *J Neurochem.* 2004;89(1):124-133. doi:10.1046/j.1471-4159.2003.02299.x
20. Chen JH, Ou HP, Lin CY, et al. Carnosic acid prevents 6-hydroxydopamine-induced cell death in SH-SY5Y cells via mediation of glutathione synthesis. *Chem Res Toxicol.* 2012;25(9):1893-1901. doi:10.1021/tx300171u
21. Drechsel DA, Patel M. Role of reactive oxygen species in the neurotoxicity of environmental agents implicated in Parkinson's disease. *Free Radic Biol Med.* 2008;44(11):1873-1886. doi:10.1016/j.freeradbiomed.2008.02.008
22. Soyer Z, Uysal S, Parlar S, Tarikogullari Dogan AH, Alptuzun V. Synthesis and molecular docking studies of some 4-phthalimidobenzenesulfonamide derivatives as acetylcholinesterase and butyrylcholinesterase inhibitors. *J Enzyme Inhib Med Chem.* 2017;32(1):13-19. doi:10.1080/14756366.2016.1226298



Scheme 1. Synthesis pathway of compounds 1-12

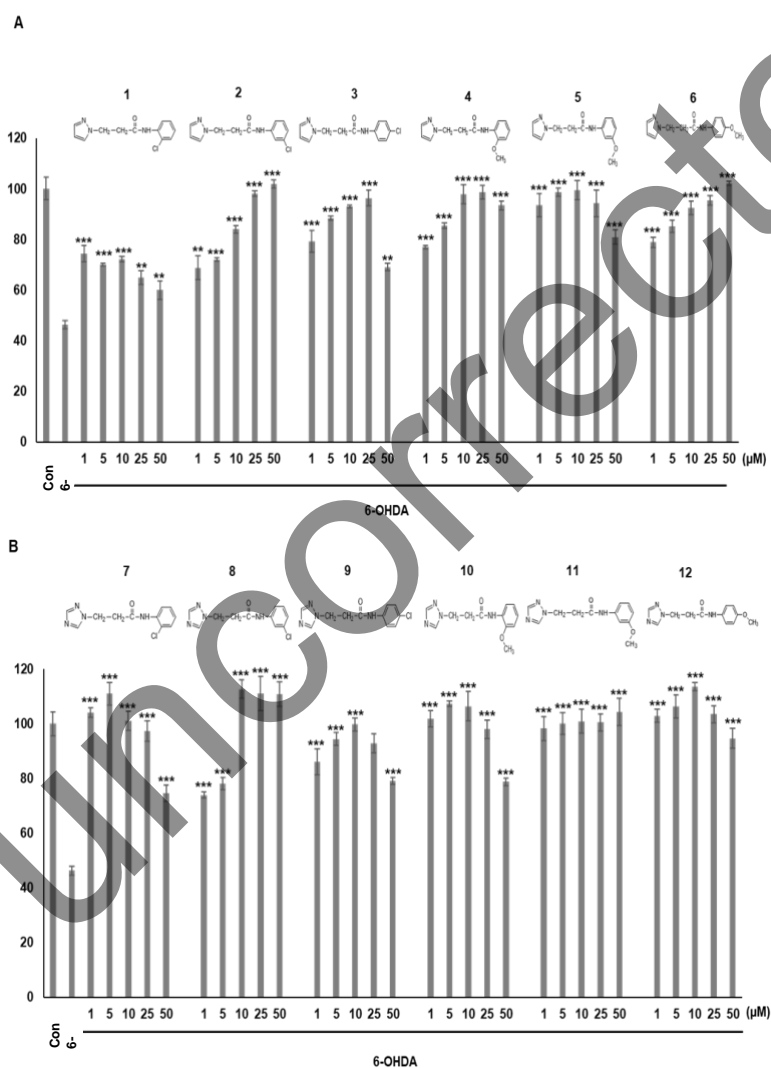


Figure 1. Synthesized compounds protect cells against 6-OHDA induced toxicity. SH-SY5Y cells were pre-treated with increasing doses of compounds for 12 h then treated with 6-OHDA for 12 h. The viability of cells was performed by WST-1 reagent. The absorbance of cells treated with DMSO as solvent control was considered 100% and cell viability of the applied concentrations was calculated. The WST-1 assay was performed by triplicate samples. ANOVA analysis with Dunnett's post hoc test was used to determine the significance of the differences compared to the control cells (* $p \leq 0.05$, ** $p \leq 0.001$, *** $p \leq 0.005$).

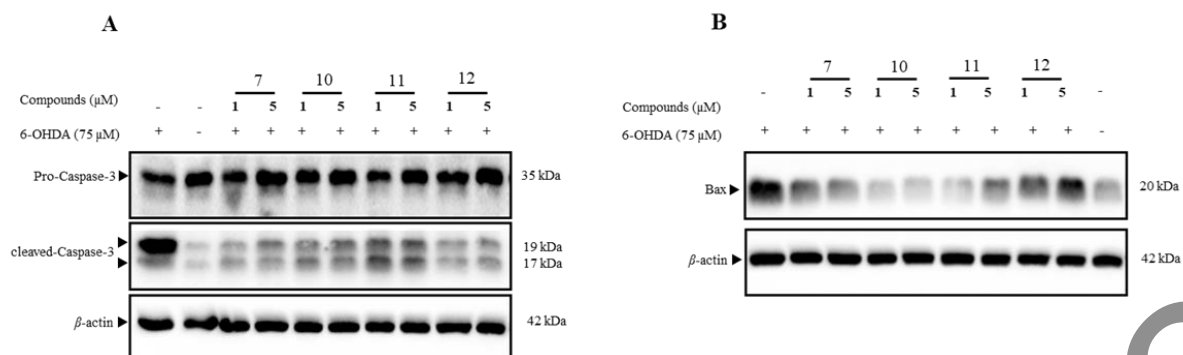


Figure 2. Selected compounds prevent 6-OHDA-induced neurotoxicity. SH-SY5Y cells were firstly treated with desired concentration of selected compounds, then treated with 6-OHDA. While DMSO was used as a solvent control; 6-OHDA was used as positive control which led to activate the cleavage form of caspase-3 and increase the level of Bax. The levels of pro-caspase 3, cleavage-caspase 3, and Bax were determined by WB using antibodies against them. β -actin was used as a loading control. The experiments were repeated three times independently; with one representative result shown.

1:

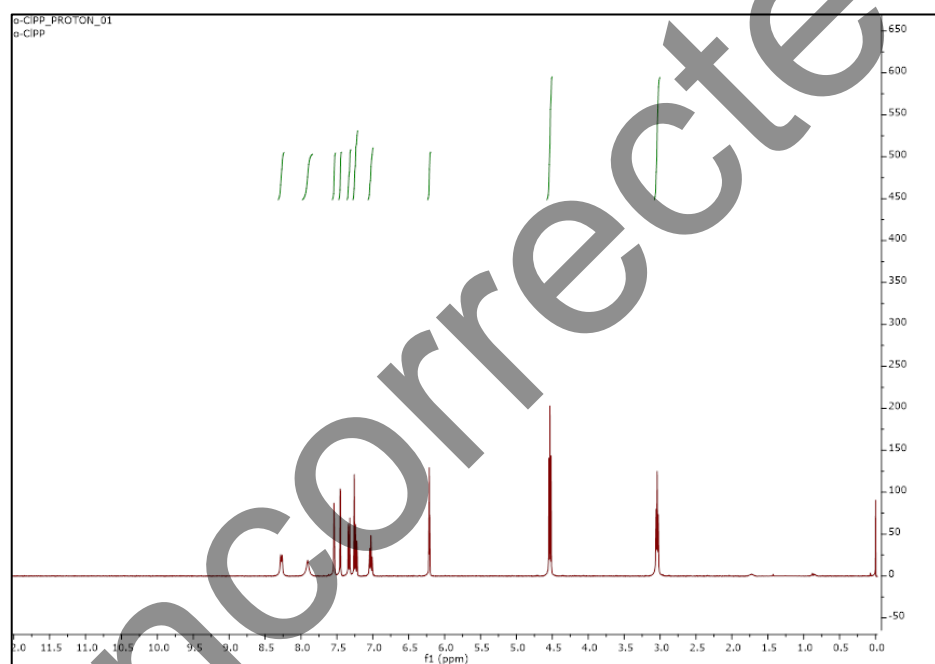
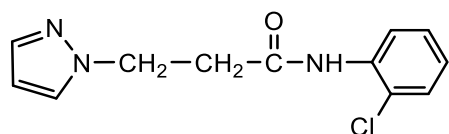


Fig. S1. ^1H NMR Spectra of **1**

2:

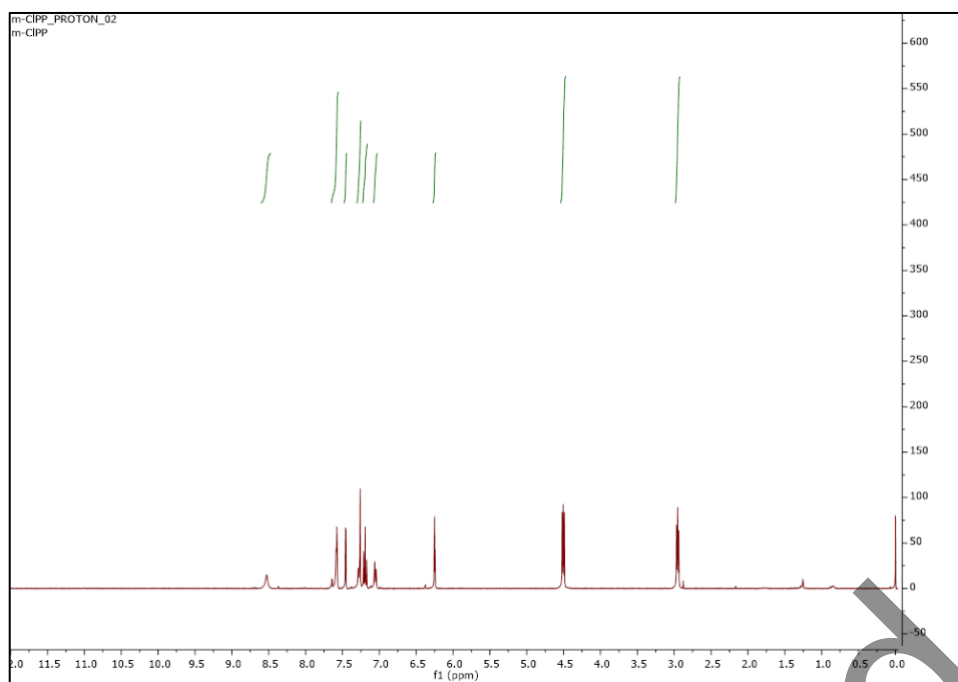
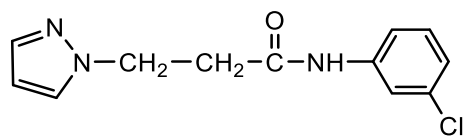


Fig. S2. ¹H NMR Spectra of 2

Uncorrected proof

3:

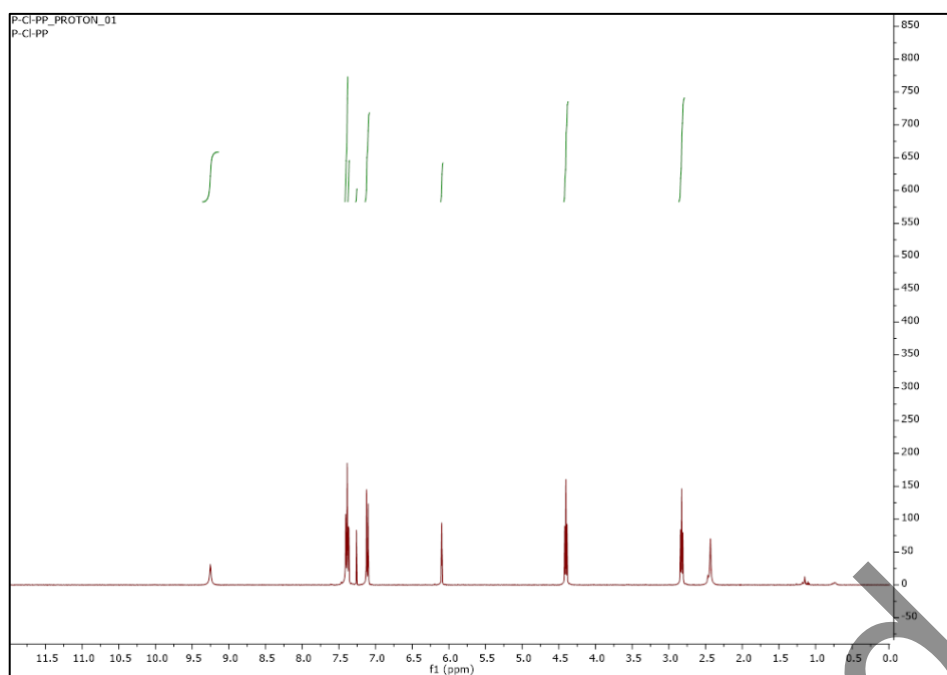
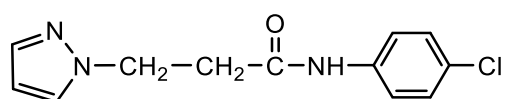


Fig. S3. ¹H NMR Spectra of 3

4:

Uncorrected proof

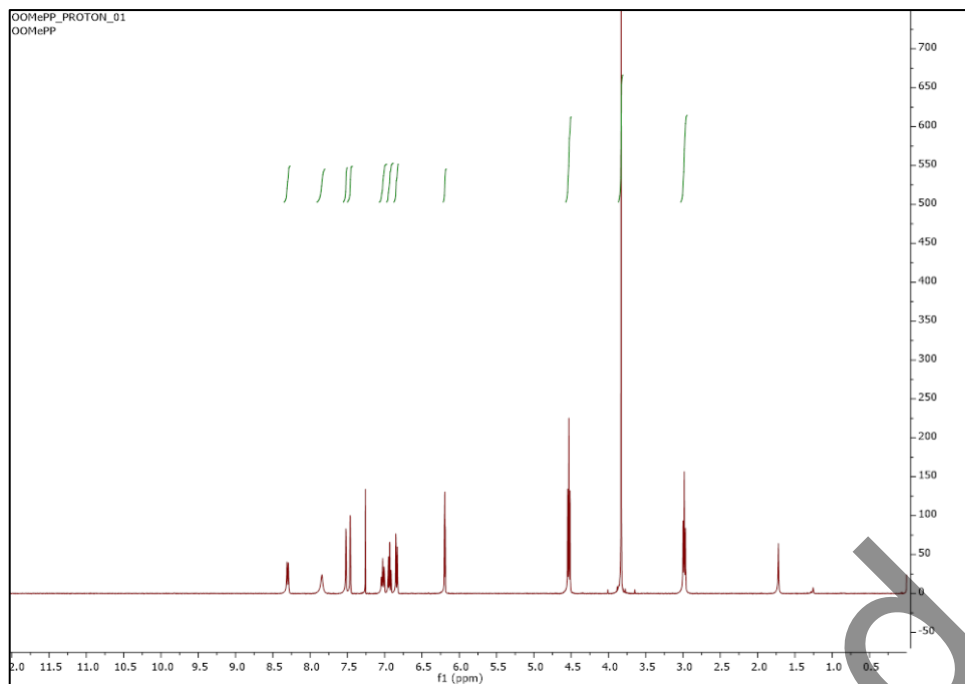
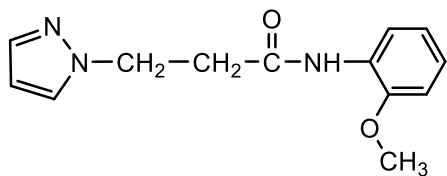


Fig. S4. ^1H NMR Spectra of **4**

Uncorrected proof

5:

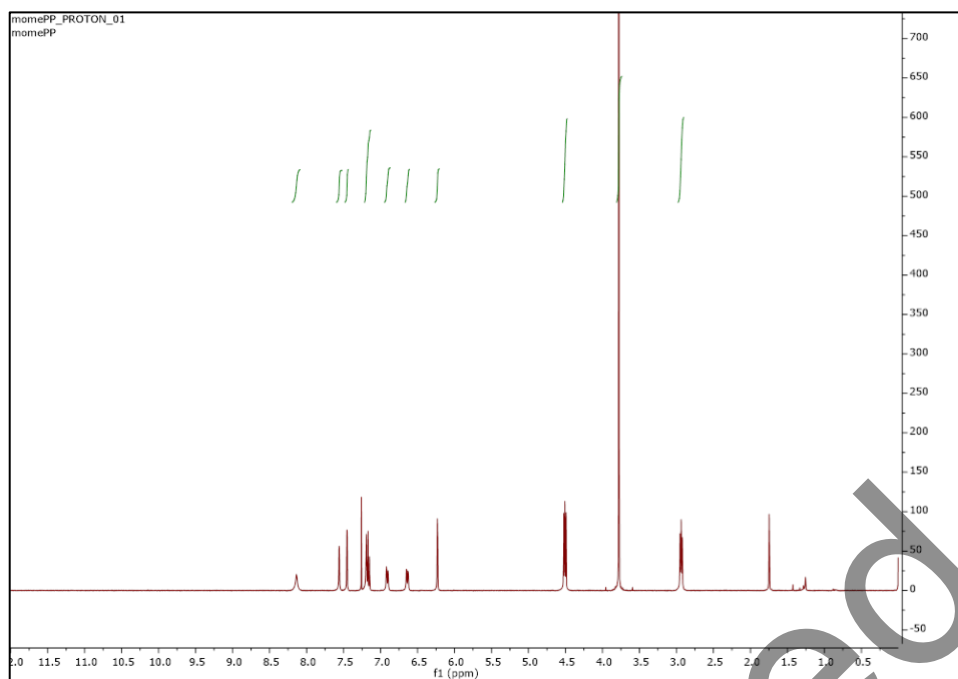
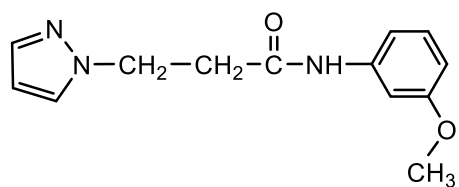


Fig. S5. ¹H NMR Spectra of 5

6:

Uncorrected proof

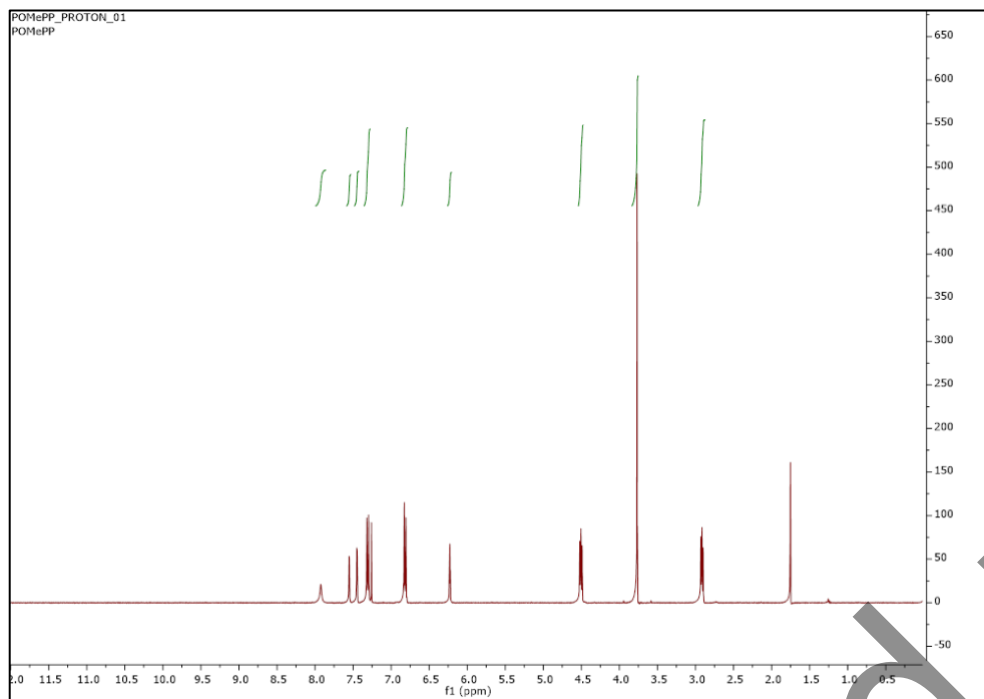
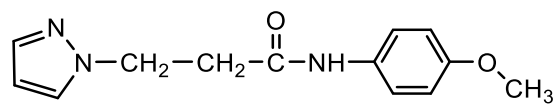


Fig. S6. ¹H NMR Spectra of 6

Uncorrected proof

7:

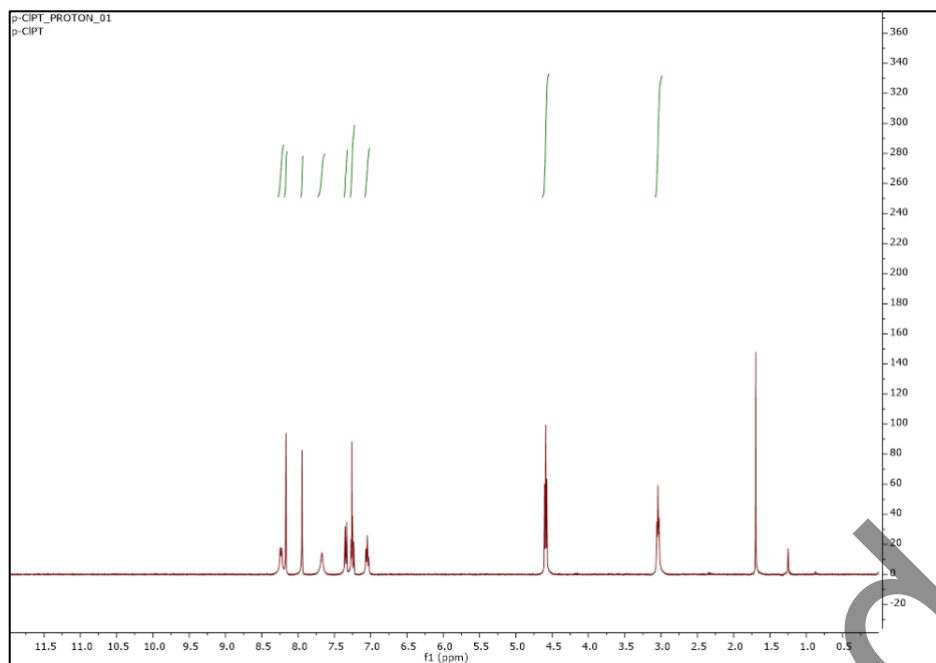
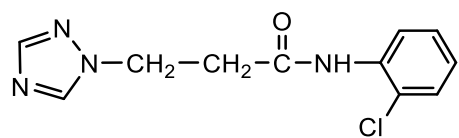


Fig. S7. ¹H NMR Spectra of 7

8:

Uncorrected proof

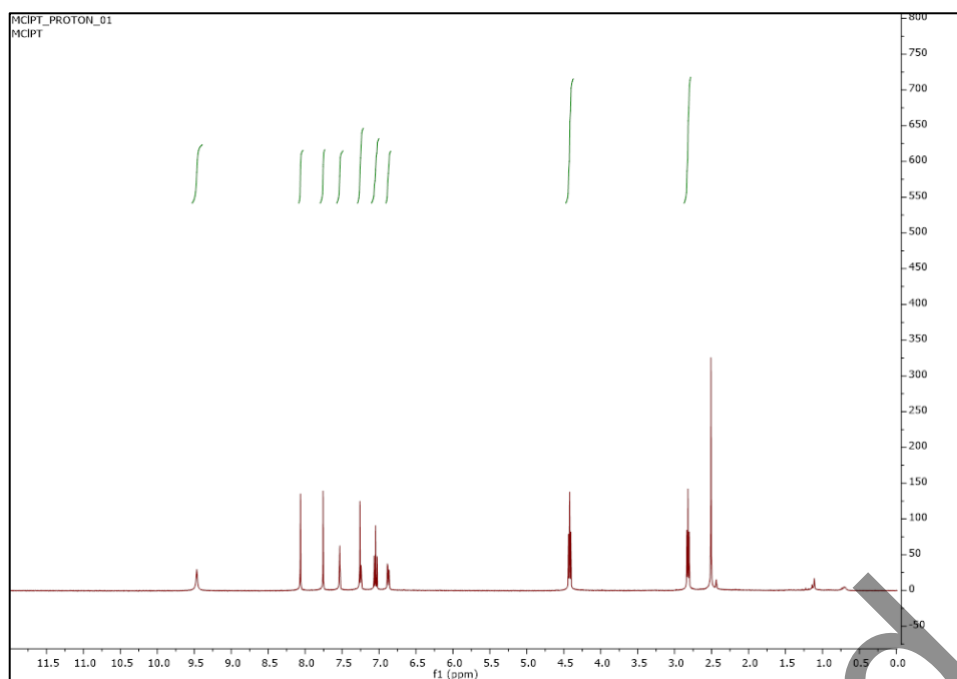
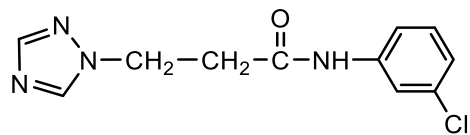


Fig. S8. ¹H NMR Spectra of **8**

Uncorrected proof

9:

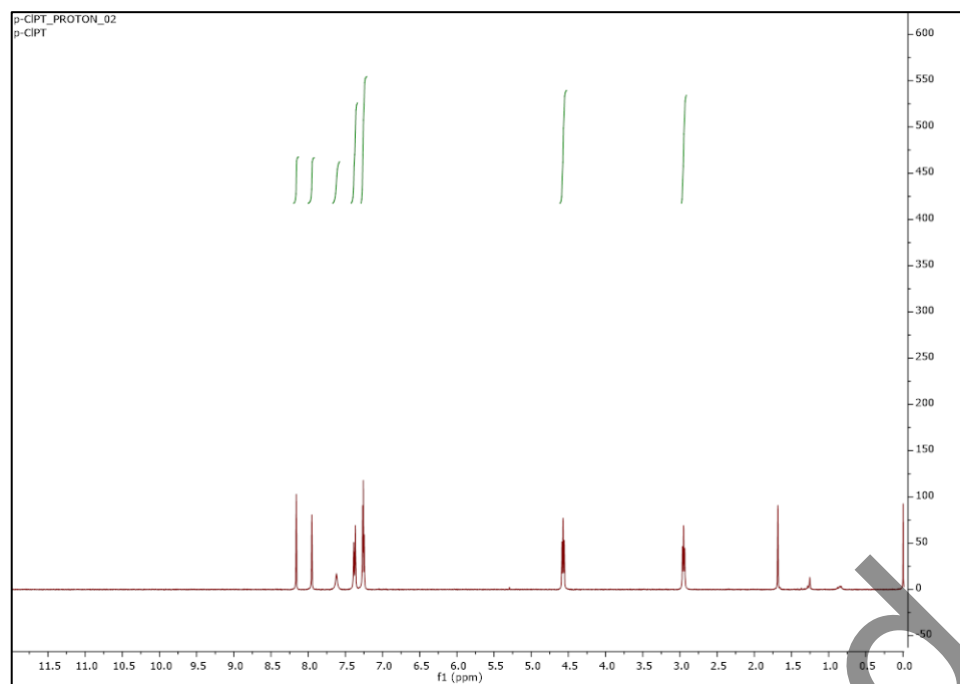
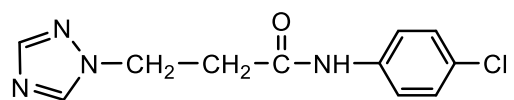


Fig. S9. ¹H NMR Spectra of 9

10:

Uncorrected proof

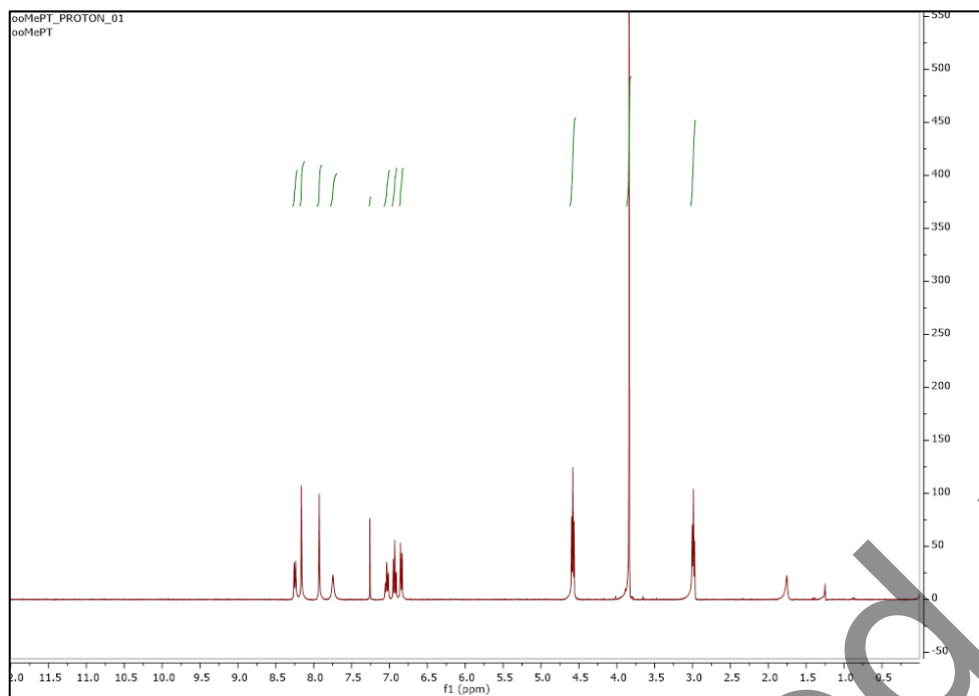
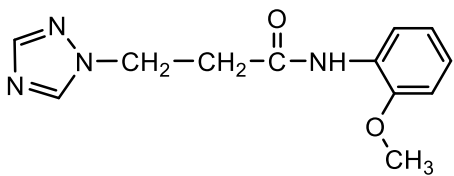


Fig. S10. ¹H NMR Spectra of 10

Uncorrected proof

11:

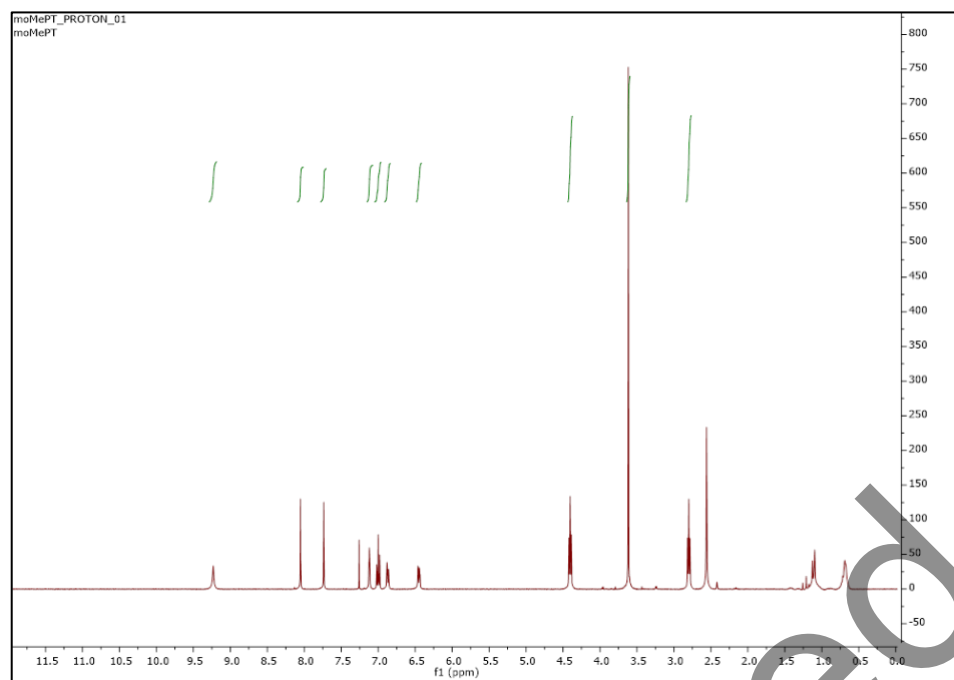
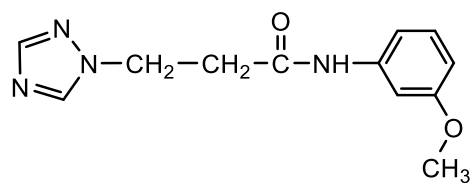


Fig. S11. ¹H NMR Spectra of 11

12:

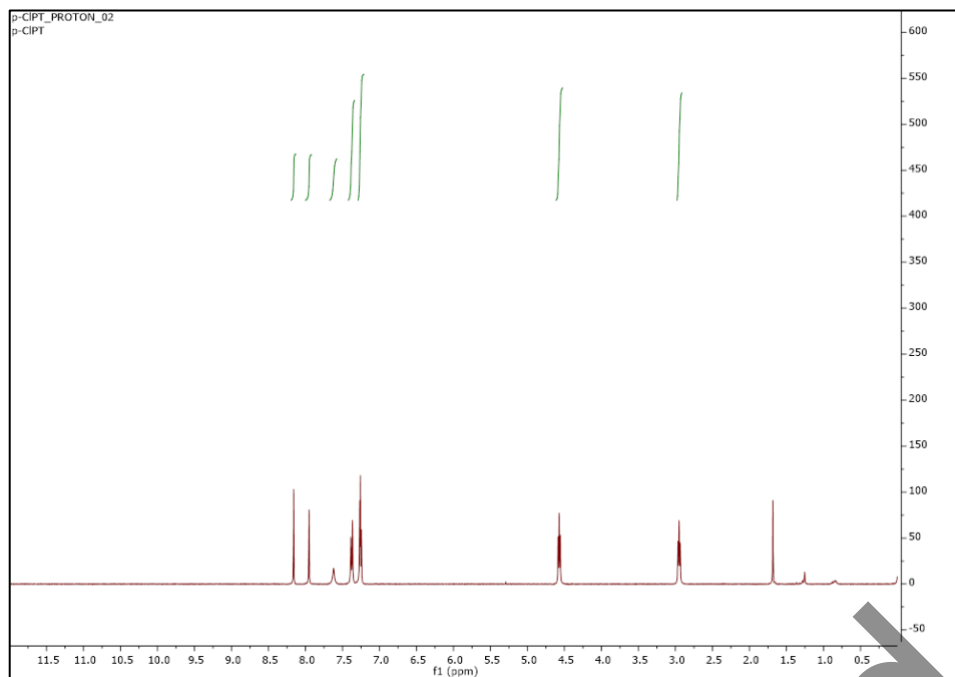
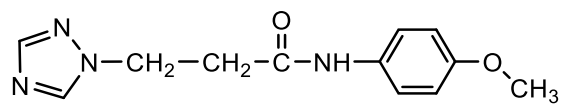


Fig. S12. ¹H NMR Spectra of **12**

Uncorrected proof

Table S1. Cell viability values of all the compounds at studied concentrations

Compound	Concentration (μM)	Cell viability (%)	Compound	Concentration (μM)	Cell viability (%)
1	<u>1</u>	74.40 \pm 0.76	7	<u>1</u>	104.33 \pm 3.77
	<u>5</u>	70.09 \pm 1.44		<u>5</u>	111.12 \pm 3.02
	<u>10</u>	72.40 \pm 2.42		<u>10</u>	101.28 \pm 3.53
	<u>25</u>	65.00 \pm 3.26		<u>25</u>	97.56 \pm 4.20
	<u>50</u>	59.92 \pm 1.97		<u>50</u>	74.79 \pm 3.38
2	<u>1</u>	68.90 \pm 2.07	8	<u>1</u>	74.03 \pm 2.04
	<u>5</u>	71.86 \pm 0.95		<u>5</u>	78.32 \pm 3.23
	<u>10</u>	84.07 \pm 1.50		<u>10</u>	113.02 \pm 4.73
	<u>25</u>	98.28 \pm 3.16		<u>25</u>	111.03 \pm 1.48
	<u>50</u>	101.98 \pm 1.97		<u>50</u>	111.20 \pm 5.20
3	<u>1</u>	79.43 \pm 3.53	9	<u>1</u>	86,08 \pm 0.61
	<u>5</u>	88.47 \pm 1.80		<u>5</u>	94,60 \pm 2.51
	<u>10</u>	93.09 \pm 2.51		<u>10</u>	100.00 \pm 3.85
	<u>25</u>	96.31 \pm 0.70		<u>25</u>	92.95 \pm 0.90
	<u>50</u>	69.09 \pm 0.98		<u>50</u>	79.20 \pm 1.95
4	<u>1</u>	77.09 \pm 2.31	10	<u>1</u>	101.97 \pm 3.11
	<u>5</u>	85.45 \pm 1.60		<u>5</u>	107.54 \pm 2.25
	<u>10</u>	97.76 \pm 4.37		<u>10</u>	106.36 \pm 0.67
	<u>25</u>	98.60 \pm 3.51		<u>25</u>	98.36 \pm 4.57
	<u>50</u>	93.62 \pm 3.38		<u>50</u>	78.92 \pm 2.78
5	<u>1</u>	93,47 \pm 0.48	11	<u>1</u>	98.60 \pm 5.20
	<u>5</u>	98.78 \pm 2.23		<u>5</u>	100.43 \pm 4.98
	<u>10</u>	99.68 \pm 4.04		<u>10</u>	101.15 \pm 4.13
	<u>25</u>	94.46 \pm 4.93		<u>25</u>	100.56 \pm 2.02
	<u>50</u>	81.05 \pm 2.97		<u>50</u>	104.35 \pm 2.26
6	<u>1</u>	78.95 \pm 2.70	12	<u>1</u>	103.07 \pm 2.24
	<u>5</u>	85.26 \pm 2.51		<u>5</u>	106.49 \pm 2.59
	<u>10</u>	92.65 \pm 4.02		<u>10</u>	113.69 \pm 2.14
	<u>25</u>	95.43 \pm 1.54		<u>25</u>	103.57 \pm 1.01
	<u>50</u>	102.21 \pm 2.26		<u>50</u>	94.93 \pm 3.92

Uncorrected proof